R.T.J McAteer

CUME #387

This exam has a total of 100 available points. It is based on concepts of solar flare emission (Q1; 25 points), magnetic field instrumentation (Q2; 40 points) and solar flare energies (Q3; 35 points) as discussed in the accompanying paper by Schrijver, ApJL, 655, L117. You do not have to read the paper in detail, but you should spend 10 minutes reading the abstract and making yourself familiar with the figures and conclusions.

There are 100 total points available. A grade of 70% is expected to be a passing grade.

Calculators are only to be used for calculations. Show all work for full points. Attempt all parts of all questions. Take a new page for each part of each question.

Constants and Equations.

1AU = 215 Solar radii By definition, 1 Mx cm⁻² =1 G Bohr magneton, $U_B = 9.27 \times 10^{-21}$ ergs G-1 Planck constant, $h = 6.63 \times 10^{-27}$ erg s Speed of light, $c = 3 \times 10^8$ m s⁻¹ Ampere's law, $\nabla X B = \mu_0 J$ By conversion, 1 Joule = 10^7 ergs Boltzmann constant, $k_B = 1.38 \times 10^{-16}$ erg K⁻¹ E_{Thermal} ~ 3NK_BT, for a population of N particles at temperature T(K) 1: This question is about the basis of a black body spectrum, as applied to solar data discussed in the paper. **There are 25 points available for this question.**

The Planck intensity of a black body spectrum is

$$B_{\lambda}(T) = rac{2hc^2}{\lambda^5} rac{1}{e^{rac{hc}{\lambda k_{
m B}T}} - 1}$$

- (a) On one set of axes, provide a sketch of the black body spectrum of the Sun (5500K), an M star, and a B star. Ensure you label the axes, including the approximate locations of the visible red edge, visible blue edges, UV range and IR range
- (b) The author comments on using both optical data (MDI, centered on 6768Å) and UV data (~1600Å). Calculate the ratio of the intensities of a black-body Sun (T=5500K) at these wavelengths.

10 points

(c) Comment on the implication of your result in 1(b) for the change from a solar absorption spectrum in the photosphere to the emission line spectrum in the corona.

5 points

(d) The solar constant is 10²⁶ W, whereas a solar flare produces 10²¹W. Why are solar flares observable, at all, above background solar emission? (2 points)

Comment on why TRACE and GOES can easily observe solar flares. (1 point) Comment on the visibility of similar sizes of flares on a B star. (2 points) (HINT: You may wish to reference your sketch to Q1(a) above)

5 points

- 2. The paper discusses selection effects and limitations that arise from the instrumentation available for the study. **There are 40 points available for this question.**
 - (a) SOHO MDI creates magnetograms using the 'normal' Zeeman effect. A single atomic transition creates a spectral line at wavelength λ_0 . With a magnetic field present, this is split into two upper energy levels.
 - (i) By assuming the resulting energy split is governed by the equation for a Bohr magneton ($\Delta E = U_B B$), where B is magnetic field (G), show that the equation (in cgs) for the wavelength separation of the two resulting spectral lines is

 $\Delta\lambda \sim 5 \times 10^{-5} \text{ B } \lambda_0^2$ (HINT Use the equation of finite differences, whereby $\Delta v = (dv/d\lambda) \Delta\lambda$ 10 points

(ii) Show that the resolving power (i.e., of the spectral resolution) of MDI at its noise level (14G, see figure 2 caption) is about 107

10 points

(iii) Future instruments plan to use an IR line of MgI at 12 μ m. Show that resolving power varies as λ^{-1} and so calculate how much less resolving power is required for this IR line, as compared to MDI.

10 points

(iv) Why is this future IR instrumentation easier in space-based instruments, as opposed to ground-based instruments?

2 points

- (b) MDI provides longitudinal, line-of-sight, magnetograms, which has provided the author with some problems.
 - (i) Galileo used concepts of foreshortening and rate of motion near the limb to prove that Sunspots were actual solar features and not the effect of an interior planet. With the aid of sketches, explain how Galileo used these two concepts to show this.

4 points

(ii) Foreshortening and rate of motion are 2 reasons why the author only uses data 'within 45 degrees of disk center' (first paragraph section 2). State one further reason, specifically related to magnetograms

2 points

(iii) With reference to Ampere's law, how come 'LOS magnetograms do not allow the measurement of electric currents' (middle of 2nd paragraph of introduction)?

2 points

- 3. The paper shows that the energy to power a solar flare is likely stored in the magnetic field close to strong magnetic gradients. In this question, we discuss three different estimates of this flare energy. **There are 35 points available for this question.**
 - (a) The GOES spacecraft measures X-ray flux at Earth. By considering a GOES X-class flare (See figure 3 for details of the flux from an X-class flare), with a duration of about 3 hours, show that the total energy emitted at the Sun during an X-class flare is about 10³² ergs. Assume an Xray production efficiency of 1 part in 10⁵

(HINT: consider the units of GOES Xray flux, and its distance of 1AU)
(HINT: At the beginning of Section 3 the authors claim a flare area corresponding to 160px in MDI images and state the conversion factor of pixels to cm.)

10 points

(b) In the penultimate paragraph of Section 3, the author shows that the magnetic field near strong magnetic field gradients can carry 10³⁰ -10³² ergs, sufficient to power major solar flares. Explain his derivation and explicitly carry out the calculation to show he is correct.

(HINT: Consider magnetic energy density ~ B²/4π)

10 points

(c) The total energy in a solar flare can also be estimated by considering the thermal emission in the corona (i.e., EUV radiation as discussed in Section 1).

(i) Show that the temperature of the TRACE EUV emission as described in Section 1 is about 10°K

5 points

(ii) Considering a flaring plasma of thermal particles inside a semihemisphere of radius about 10 times the thickness of the emerging flux tube bundle discussed by the author (Q3b above). Show that electron densities must be about 10¹¹ cm⁻³ for an X-class flare.

10 points

A CHARACTERISTIC MAGNETIC FIELD PATTERN ASSOCIATED WITH ALL MAJOR SOLAR FLARES AND ITS USE IN FLARE FORECASTING

CAROLUS J. SCHRIJVER

Lockheed Martin Advanced Technology Center, Palo Alto, CA; schryver@lmsal.com Received 2006 November 10; accepted 2006 December 15; published 2007 January 8

ABSTRACT

Solar flares result from some electromagnetic instability that occurs within regions of relatively strong magnetic field in the Sun's atmosphere. The processes that enable and trigger these flares remain topics of intense study and debate. I analyze observations of 289 X- and M-class flares and over 2500 active region magnetograms to discover (1) that large flares, without exception, are associated with pronounced high-gradient polarity-separation lines, while (2) the free energy that emerges with these fibrils is converted into flare energy in a broad spectrum of flare magnitudes that may well be selected at random from a power-law distribution up to a maximum value. This maximum is proportional to the total unsigned flux R within ~15 Mm of strong-field, high-gradient polarity-separation lines, which are a characteristic appearance of magnetic fibrils carrying electrical currents as they emerge through the photosphere. Measurement of R is readily automated, and R can therefore be used effectively for flare forecasting. The probability for major flares to occur within 24 hr of the measurement of R approaches unity for active regions with the highest values of R around R around R can be regions with $R \leq 10^{19}$ Mx, no M- or X-class flares occur within a day.

Subject headings: Sun: flares — Sun: magnetic fields

1. INTRODUCTION

Solar flares are known to occur preferentially in magnetic regions with strong field gradients, long polarity-inversion lines, complex polarity patterns, or sunspot umbrae containing both polarities within a common penumbra. Searches for discriminants between flare-producing and flare-quiet regions have thus far resulted only in trends or ambiguous findings (see Leka & Barnes 2003a, 2003b and references therein). It has been found, however, that the emergence of electrical currents embedded in magnetic flux, rather than surface shear flows or other purely atmospheric effects, appears to be key in driving active region flaring (e.g., Wheatland 2000a; Démoulin et al. 2002a, 2002b; Schrijver et al. 2005; Leka & Barnes 2003a. 2003b; Jing et al. 2006; Falconer et al. 2002). These strong electrical currents do not persist for more than about a day (e.g., Pevtsov et al. 1994; Schrijver et al. 2005) unless sustained by continued flux emergence. It is therefore no surprise that the emergence of compact field has also been found to be positively correlated with some flaring (e.g., Schmieder et al. 1994; Wang et al. 1994; Choudhary et al. 1998; Li et al. 2000).

In order to significantly increase the sample size over those in previous studies, we must use full-disk line-of-sight (LOS) magnetograms, such as obtained by the Solar and Heliospheric Observatory (SOHO) Michelson Doppler Imager (MDI; Scherrer et al. 1995), which has observed one magnetogram every 96 minutes almost continuously since mid-1996. Although LOS magnetograms do not allow the measurement of electrical currents, they certainly can be quite revealing of their presence: a compact current, emerging through the photosphere with a magnetic field winding helically about it, would show up in cross section within the photosphere as an elongated polarity-inversion line, with narrow ridges of strong opposite-polarity fields immediately adjacent to it. This characteristic pattern for emerging currents is seen whenever the appearance of the coronal field is distinctly nonpotential (Schrijver et al. 2005), so that it appears likely that high-gradient, strong-field polarity-reversal lines in LOS magnetograms are in fact proxies of (near-)photospheric electrical currents.

In this study, I use a large sample of LOS magnetograms and introduce a new metric to find that high-gradient, strong-field polarity-separation lines—characteristic of electrical currents emerging through the photosphere—are necessary for major solar flares to occur. Based on this, I propose that the emergence of a current-carrying magnetic field causes most, if not all, major solar flares.

2. FLARE INITIATION SITES AND POLARITY-SEPARATION LINES

From the sample of 574 M- and X-class flares that were at least partly observed by the *Transition Region and Coronal Explorer (TRACE*; Handy et al. 1999), between 1998 July 14 and 2006 July 6 at 1" resolution, I select the 289 within 45° of disk center. I locate the brightest area in EUV or UV images, allowing for a delay between the start time of the X-ray flare observed by the *Geostationary Operational Environmental Satellite (GOES)* and the brightening in *TRACE* images of 1–2 ks for the 171 or 195 Å images to allow significant coronal EUV brightening to occur, or 0.5–1 ks for 1600 or 1700 Å images to see the more promptly developing flare ribbons.

To identify high-gradient polarity-separation lines, I dilate bitmaps of SOHO MDI magnetograms where either positive or negative flux densities exceed 150 Mx cm⁻² with kernels of 3×3 pixels of 2" each. Where these two maps overlap (i.e., where the product M of the two dilated bitmaps is nonzero), we find the relatively strong opposite-polarity fields that lie closer to each other than the instrument's 4" resolution.

The average distance D of the brightest TRACE (E)UV location, after resampling to 4'' pixels, to the nearest point on any such polarity-separation line within the 320×320 pixel magnetogram cutouts is 20 Mm. The distribution of D is strongly peaked at small distances: two-thirds of the cases have $D < D_{\rm sep} = 15$ Mm, while 81% lie within 30 Mm compared to typical active region sizes of 150 Mm or more. This small separation of strong-field, compact polarity-separation lines and flare initiation sites further supports the direct association of M- and X-class flares with these magnetic features.

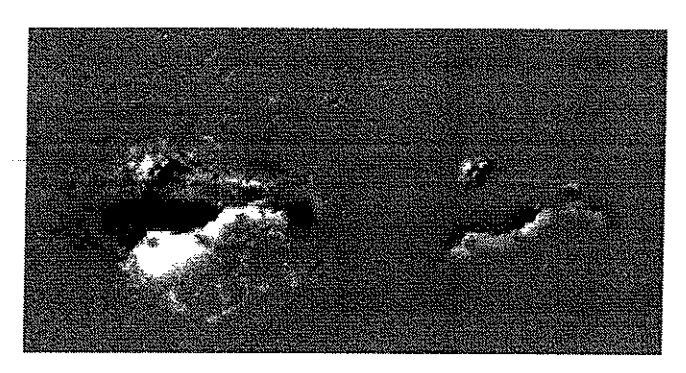


Fig. 1.—Left: Example of a SOHO MDI magnetogram (cutout of 160×160 pixels of 2" square) around the time of the M4.6 flare on 2005 September 14 10 UT (log R=5.03). Right: Magnetogram multiplied with the weighted map W of the field near high-gradient, strong-field, polarity-separation lines, which, after summing their absolute values, yields R.

3. QUANTIFYING THE FLARE DRIVER

To quantify the association of flares with flux near high-gradient, strong-field polarity-separation lines, I measure the unsigned flux R near the polarity-separation lines described above. This is done by taking the bitmap M of high-gradient strong-field polarity-separation lines described in § 2, and convolving that with an area-normalized Gaussian with a FWHM of $D_{\rm sep}=15$ Mm to obtain a weighting map. This weighting map is multiplied with the absolute value of the magnetogram; i.e., the quantity R is computed as the weighted unsigned flux density summed over all instrument pixels in a 160×160 pixel

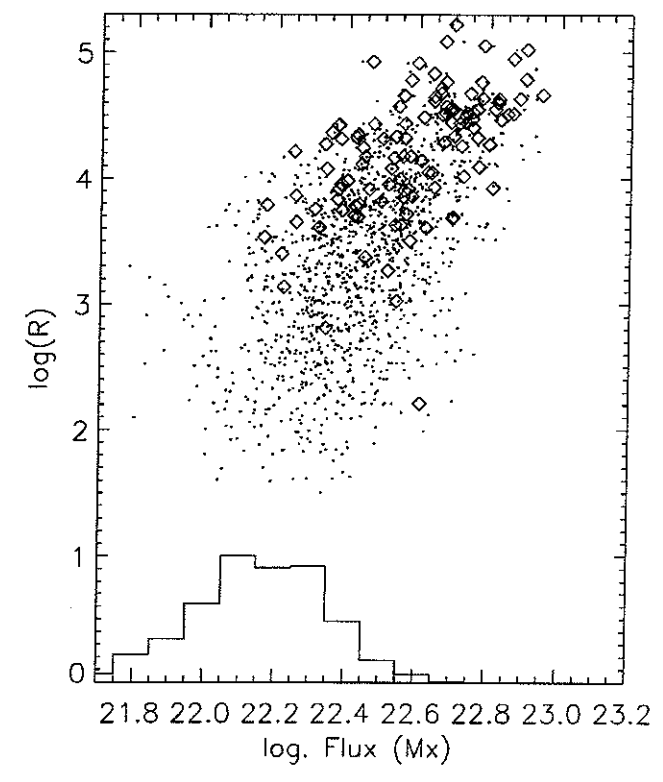


Fig. 2.—Scatter diagram of unsigned total active region fluxes vs. flux R near compact, high-gradient polarity-separation lines. Regions with M- or X-class flares are shown by diamonds, all other with $R \neq 0$ by dots. The histogram shows the peak-normalized distribution of magnetic fluxes for regions with R = 0 (i.e., with no strong-field, high-gradient polarity-separation lines). The unsigned fluxes are sums of absolute values in a 240 \times 240 pixel area (of 2" pixels) centered on the active region, corrected for a noise contribution from the 14 Mx cm⁻² single pixel noise (Hagenaar 2001).

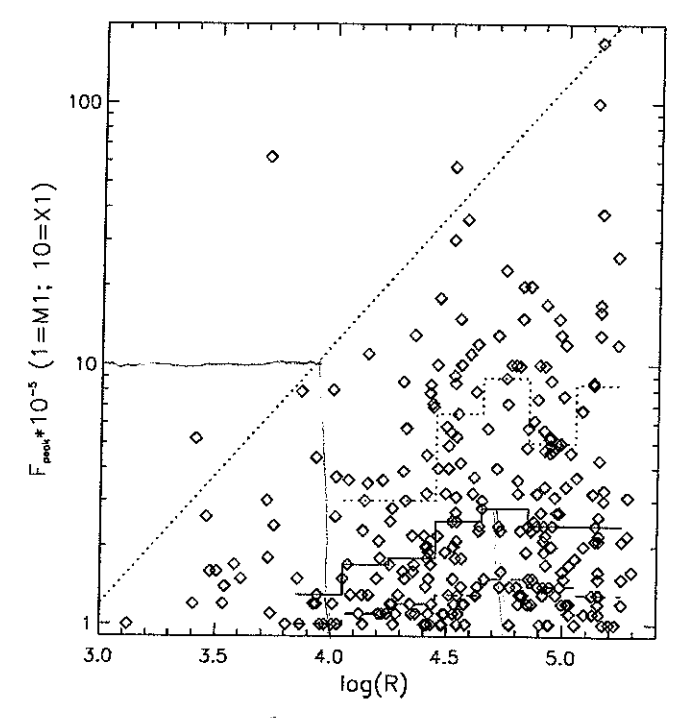


Fig. 3.—Scatter diagram of peak flare flux densities (GOES 1-8 Å passband in W m⁻²) vs. R. The histograms in this figure show the 25th, 50th, and 75th percentiles of the flare distribution as function of R. The dotted straight line at $E_{\rm resk} = 1.2 \times 10^{-8} R$ has 99% of the observed flares below it. The only flare that clearly lies above this line is an X6.2 flare that started around 2001 December 13 14:30 UT. The value of $\log R$ in this active region decreased from 4.2 half a day prior to the flare to 3.7 at the time of the flare, but at 4.2 would still lie well above the dotted line. This region has a narrow fibril of one polarity embedded within an area of strong field of the opposite polarity, which likely causes the measure R to strongly underestimate the true flux involved (see footnote). This may (in part) explain its unusual position in this diagram.

box centered on the region (see the example in Fig. 1). This algorithm turns out to result in a maximum observed value of $\log R$ of somewhat over 5; in these units, $\log R$ thus yields a convenient classification scale, as discussed below. To convert R to maxwells, multiply by the area of MDI's 2" pixels, or 2.2×10^{16} cm²; the magnetograms are calibrated as for the standard MDI level 1.5 data processing without further corrections for instrument sensitivity or nonlinearity.

The flux R is poorly correlated with the total flux in the active regions (Fig. 2; C = 0.60 for regions with R > 0). Clearly, R is a far more significant measure for major flare potential than the unsigned flux: all but one of the active regions with M- or X-class flares lie at $\log R > 2.8$, but lie spread out over most of the flux range.

A scatter diagram relating the GOES 1-8 Å peak flux density, $F_{\rm peak}$, with log R—as in Figure 3—reveals the pronounced clustering of the flares in the lower right corner of the diagram (diagrams for times up to 1 day prior to the flare are very similar). This suggests (1) that R is a measure for the maximum

¹ Fine-scale magnetic structure is, of course, weakened if not lost by the instrument resolution. This is particularly the case when a ridge of one polarity is contained within the field of the opposite polarity (as in the cases of X flares on 2001 December 13—see Fig. 3—and 2006 December 13—not included in the present sample). For example, when two Gaussian profiles of one sign bracket another profile of the opposite sign that is otherwise identical, the central peak is weakened by a factor of 3 at a separation of 2.9 σ of the outer peaks, and it disappears entirely below 1.2 σ . For such compact multireversal structures, the finite instrument resolution will cause the flux near high-gradient polarity-separation lines to be strongly underestimated.

energy available for flares in a given region $(F_{\rm peak} \lesssim 5.4 \times 10^{-20} R_{\rm Mx}$ [Fig. 3, dotted line], with $F_{\rm peak}$ in 10^{-5} ergs cm⁻² s⁻¹ [$F_{\rm peak} = 1$ for an M1 flare]), and (2) that active regions can reduce their free energy by relaxing through a series of flares, with smaller flares being much more likely than large flares.

Does the flux near strong, compact polarity-separation lines carry enough energy to power major flares? An order of magnitude estimate of the energy E is obtained by assuming that an emerging flux bundle has a thickness comparable to $D_{\rm sep}=15$ Mm and that the intrinsic characteristic field strength lies below the characteristic postemergence strength of ~ 1 kG, say, $\langle B \rangle \sim 300$ G. Because $R=\langle B \rangle A$, for area A, the energy $E(\log R=3)\sim (\langle B \rangle^2/4\pi)AD=\langle B \rangle DR/4\pi\sim 10^{30}$ ergs. The highest value corresponds to $E(\log R\approx 5.3)\sim 2\times 10^{32}$ ergs. These energies suffice to power major solar flares (e.g., Hudson 1991; Crosby et al. 1993).

When R curves as a function of time are normalized to their individual peak values, their ensemble average reveals a tendency for an increase (of $\sim 20\%$) during the 2 days prior to a major flare, followed by a decrease (of $\sim 7\%$) the following day, as expected for a measure of the flare driver. The spread about this tendency is large, but that should not be surprising: regions often flare multiple times over a period of days as flux continues to emerge.

4. FLARE LIKELIHOOD AND FORECASTING

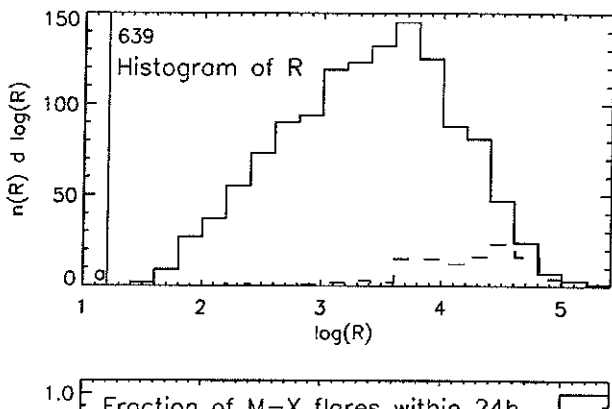
To test whether the emergence of current-carrying flux is essential to drive major flares, I select 2500 entries within 45° of disk center from the daily active region entries in the NOAA/ SEC solar region data between 1999 January 1 and 2006 October 23, during which SOHO MDI operated nominally (note that the flaring regions studied in § 3 are part of that full set, and some of these regions will have been randomly selected in the sampling of 2500 magnetogram observations). The distribution of $n(R) d \log R$ for that sample is shown in Figure 4a. No M- or X-class flares occur within 24 hr of the determination of R for $\log R < 2.8$ (61% of the sample), thus providing a useful "all clear" metric. The single apparent exception is an active region that experienced a strong decrease from $\log R = 3.3$ only 3 hr before an M1.9 flare, which may be interpreted to indicate that the emerging current had largely passed through the photosphere, then mostly embedded in the corona.

Only 9% of the active regions with $\log R > 2.8$ display M-or X-class flares within 24 hr of their observation. Figure 4b shows that the fraction of these regions with at least one major flare within 24 hr increases rapidly with R, reaching unity for $\log R \gtrsim 5.0$.

The occurrence rates of M- or X-class flares for a given R are consistent with the concept that free energy is converted to flare energy in a finite flare sequence selected randomly from a broad power-law distribution (Wheatland 2000b) in which small flares are far more frequent than large ones. The distribution of the peak flare flux densities in the GOES 1–8 Å passband for flares with $\log R > 4.8$, for example, is a power law, $F^{-\alpha} dF$ with index $\alpha \sim 1.75$. The fraction of flares with peak fluxes below F for a power-law distribution with a maximum value of F_m and minimum F_0 asymptotically approaches $f(F) \approx 1 - (F_0/F)^{\alpha-1}$ for $F_m \gg F_0$. This is consistent with the empirical percentiles in Figure 3 that level off for $\log R \gtrsim 4.5$.

5. FLARING AND NEWLY EMERGING REGIONS

In order to study how newly emerging active regions behave compared to randomly sampled active regions, I identify all



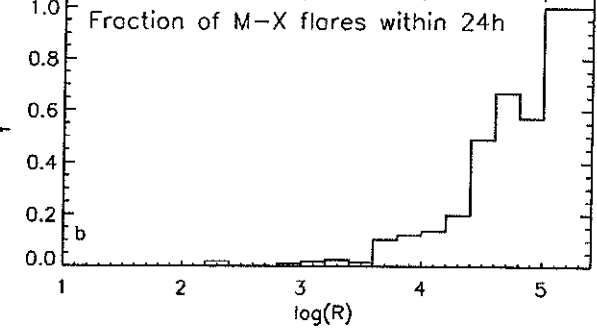


Fig. 4.—(a) Histogram of fluxes R near compact, high-gradient polarity separation lines for a random sample of 2500 active region magnetograms (solid line), and for the subset with M- or X-class flares within 24 hr of their observation (dashed line). The 639 regions with R=0 (i.e., with no strong-flux) gradient polarity-separation lines) are shown at $\log R \equiv 1$. (b) Ratio of the two histograms showing the fraction of all regions with an M- or X-class flare within 24 hr.

active regions in the period 1998 through 2005 that were first listed in the NOAA catalogs between E45 and E00, existed as a numbered region for at least 4 days, and reached a size larger than 40 microhemispheres. From that list, I select isolated regions (no neighboring region within 3') and require that all M- and X-class flares, if any, that occurred on the day before first listing and the two subsequent days were assigned solar coordinates to eliminate ambiguity in whether the region produced major flares or not. Only 38 active regions meet these criteria.

Of the 12 regions with max $(\log R) \le 3.0$ during the first 3 days of their existence, none showed an M- or X-class flare, consistent with the 0.19% probability of major flaring in the sample of 2500 randomly selected active region magnetograms with such low values of R. For $3.1 \le \max(\log R) \le 4.0$, two in 21 regions $(10\% \pm 7\%)$ showed major flares, consistent with the 5.7% in the larger random sample. Of the five regions with max $(\log R) \ge 4.1$, one exhibited a major flare (expected in 31% of realizations of such a small sample with a flare likelihood of 30% as in the larger random sample).

Although the sample of emerging regions is small, I conclude that there is no significant difference in the likelihood of major flaring as a function of R between emerging and existing active regions. It therefore appears that it is not the mere fact of flux emergence that drives flaring or causes a nonzero value of R but rather that the pattern of such flux emergence is the determining factor in whether major flares occur or not.

6. DISCUSSION AND CONCLUSIONS

This study establishes that major solar flares of class M or X are invariably associated with the emergence of flux that

TABLE 1
FLARE PROBABILITIES

CLASS	Probability					
	$\log R \approx <3.0$ (%)	$\log R \approx 3.0$ (%)	$\log R \approx 3.5$ (%)	$\log R \approx 4.0$ (%)	$\log R \approx 4.5$ (%)	$\log R \approx 5.0$ (%)
>M1		2	5	12	50	~80
>M3		~0	<1	3	20	35
>X1		0	~0	~1	10	20
>X3		0	0	~0	i	1-2
Maximum	<c9< td=""><td><m1< td=""><td><m4< td=""><td><x1< td=""><td><x4< td=""><td><x10< td=""></x10<></td></x4<></td></x1<></td></m4<></td></m1<></td></c9<>	<m1< td=""><td><m4< td=""><td><x1< td=""><td><x4< td=""><td><x10< td=""></x10<></td></x4<></td></x1<></td></m4<></td></m1<>	<m4< td=""><td><x1< td=""><td><x4< td=""><td><x10< td=""></x10<></td></x4<></td></x1<></td></m4<>	<x1< td=""><td><x4< td=""><td><x10< td=""></x10<></td></x4<></td></x1<>	<x4< td=""><td><x10< td=""></x10<></td></x4<>	<x10< td=""></x10<>

Notes.—Likelihood of major (X or M) flares within 24 hr of the determination of the unsigned, weighted magnetic flux R within 15 Mm of high-gradient, strong-field polarity-separation lines. Also listed is the maximum expected flare class.

displays strong-field, high-gradient polarity-separation lines. The likelihood of such flares to occur does not appear to depend on whether this flux is newly emerging into the quiet network or whether it is emerging into a preexisting active region. Such a field pattern is characteristic of compact electrical currents emerging through the solar surface. I therefore propose that major solar flares occur because of the release of energy associated with the emergence of compact electrical currents into the solar atmosphere, rather than, for example, as a result of the interaction of flux systems or the buildup of stresses by surface flows.

The data support the notion that energy associated with the emergence of flux with compact high-gradient, strong-field polarity-separation lines is dissipated in a series of flares whose energies are drawn randomly from a power-law distribution that extends up to a maximum value set by the available energy. For regions with more energy (as measured by the measure R introduced here), the power-law distribution of flare strengths maintains its slope but is scaled upward so that the frequency of flares of all possible magnitudes increases while the cutoff for the maximum flare magnitude grows. Thus, with increasing R, the probability of a region to produce a major flare (shown in Fig. 4b) increases both because larger flares become possible and because flares of all magnitudes become statistically more frequent.

The consequences of the observations discussed here for flare forecasting are quantified in the conditional flare probabilities in Table 1 that combine the statistics of flare magnitudes with the overall flare likelihoods shown in Figures 3 and 4. Forecasts will remain probabilistic unless we can learn what determines

the energy release for a specific flare given the active region field. We may, of course, find that the flare process is like a sandpile avalanche system in which small perturbations lead to a broad range of intrinsically nondeterministic responses. To establish whether or not this is the case, we need to observe a large sample of flares with next-generation high-resolution solar instrumentation. Only such a large sample will contain the information needed to reveal the trends hidden in the statistical processes, as demonstrated by this study based on 8 yr of SOHO, TRACE, and GOES records. This argues not only in favor of obtaining long data records to build large statistical samples but also for a discovery infrastructure in the form of easily searchable, multi-instrument knowledge bases.

I thank the TRACE planner team (Monica Bobra, Ed DeLuca, Brian Handy, Jack Ireland, Patricia Jibben, Charles Kankelborg, LiWei Lin, David McKenzie, Rebecca McMullen, Dawn Myers, Kathy Reeves, Alana Sette, Dick Shine, Ted Tarbell, Harry Warren, Mark Weber, Meredith Wills-Davey, Trae Winter, and Jake Wolfson) for their diligence over the years in observing flareimminent active regions; Kathy Reeves and Patricia Jibben for maintaining the TRACE flare catalog at SAO; Zoe Frank for conscientiously bringing MDI magnetograms into our archive; Sam Freeland for maintaining the indispensable SolarSoft IDL routines; the NOAA/SEC team for their untiring recording of all solar flares; and Bart De Pontieu and the referee for help in refining the conclusions and their presentation. This work was supported by NASA under the TRACE contract NAS5-38099 with NASA Goddard Space Flight Center and MDI-SOI contract NASS-30386 with NASA through Stanford contract PR 9162.

REFERENCES

Choudhary, D. P., Ambastha, A., & Ai, G. 1998, Sol. Phys., 179, 133 Crosby, N. B., Aschwanden, M. J., & Dennis, B. R. 1993, Sol. Phys., 143,

Démoulin, P., Mandrini, C. H., Van Driel-Gesztelyi, L., Lopez Fuentes, M. C., & Aulanier, G. 2002a, Sol. Phys., 207, 87

Démoulin, P., Mandrini, C. H., van Driel-Gesztelyi, L., Thompson, B. J., Plunkett, S., Kovári, Z., Aulanier, G., & Young, A. 2002b, A&A, 382, 650 Falconer, D. A., Moore, R. L., & Gary, G. A. 2002, ApJ, 569, 1016

Hagenaar, H. J. 2001, ApJ, 555, 448

Handy, B. N., et al. 1999, Sol. Phys., 187, 229

Hudson, H. S. 1991, Sol. Phys., 133, 357

Jing, J., Song, H., Abramenko, V., Tan, C., & Wang, H. 2006, ApJ, 644, 1273

Leka, K. D., & Barnes, G. 2003a, ApJ, 595, 1277

———. 2003b, ApJ, 595, 1296

Li, H., Sakurai, T., Ichimoto, K., & UcNo, S. 2000, PASJ, 52, 465

Pevtsov, A. A., Canfield, R. C., & Metcalf, T. R. 1994, ApJ, 425, L117

Scherrer, P. H., et al. 1995, Sol. Phys., 162, 129

Schmieder, B., et al. 1994, Sol. Phys., 150, 199

Schrijver, C. J., De Rosa, M. L., Title, A. M., & Metcalf, T. R. 2005, ApJ,

Wang, T., Xu, A., & Zhang, H. 1994, Sol. Phys., 155, 99

Wheatland, M. S. 2000a, ApJ, 532, 616

———. 2000b, ApJ, 532, 1209

Solutions gener stype - list ise, I'm decay En peds mid visible Correct lobely UV, Vo, VR, IR

6) PZ 6768A) to Fellow gans Pt_ is 200 hindred

3 points As the or backgrand is so much weather spectral lines is higher, bother bachgand thromosphere and covona in emission below MISCO A 2 points - Che chram [car

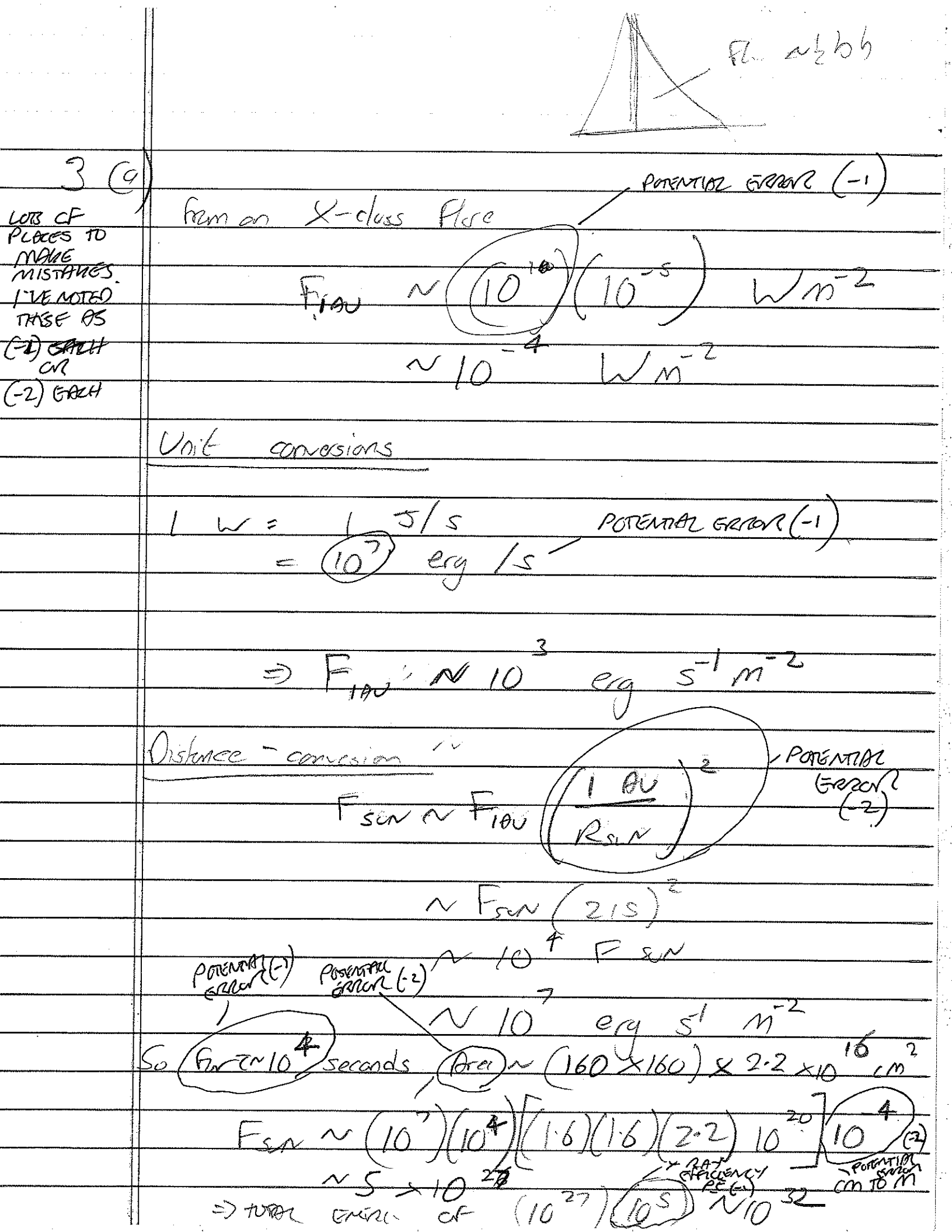
- Most of 10th is in optical Most Place energy is in U 500 where the block budy spectrum is much Janes Aprilos - ECE observes in X-rogs where bachgrandis very law and change in intensity is high 2 pointes Student may B-ster, meh highe U.EUV buchgand Here publy not visible in their Figure. bit higher volus For notter stor.

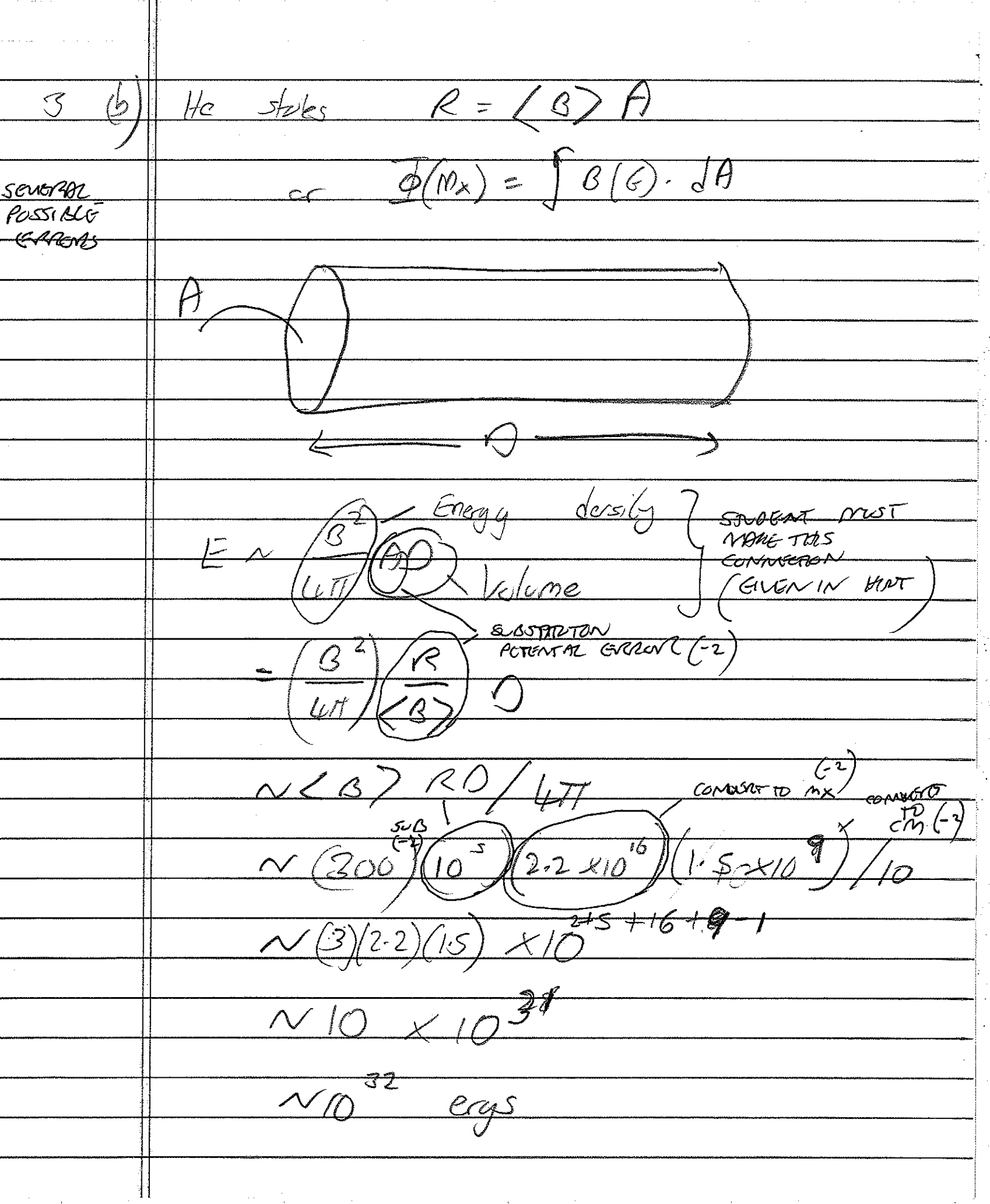
TOG HOTEMEN SOURCE GRADRS. PSTOCK WHO MUSES 1275 MA-1 65 BX NXB POINTS 5 POINTS TO 66 ms FAVE CORRESTY POKMIM SURCE & ENCOR 5 PUNTS,

(ii POTENTIAL SUMPLE of CRACK wito DO STUDENTS MOT VOE WILL BE INCOMPLET STATINES LAW THE PORENTAL SC ST GREROR UNITS (SUBNAGET 3

2 SPAMS FED CONDITON SPUM3 TOHENG 0.67

3001	
2 (6) (1)	in Earth's chausphere termono
	in Earth's chousphore kernono
1	
(b)	
J	[B] G'eld is rodiel = [less [B]) measured
rchinant Hamma Parker Observans Herback (2000 cc) (1000 cc) (1000 cc)	2 Nitsons
	also area is (Exestratered)
·	(i) Sunspols elliptical planets renain rund
2 POINTS FOR	
L PUNTS FER	- Suppols slaver at limb, plunets not slaver
30,0,0	Slaver
· · · · · · · · · · · · · · · · · · ·	(ii) B TXB=465
···········	a de la
	estimate 5 Ex, By and B2 6 VE pares
	estimate 5
	=) las only provide (I of these)
	*
i	





1=171 ×10 6m E = & N UBT ~ (6.63 ×10°) 3×10° N10 +10 5

Emer N3NKT (V) ~30KT (VHEMISPHERE ~36) (1.4×10-10) (10) (2) (3) (1) (1036) semi-banisphare, radio RN 10Mm 10-16+6+30 =) 1 N 10" cm-3 For EN 1032 egs